

# A Directional Dogbone Flextensional Sonar Transducer

Stephen C. Butler

Naval Undersea Warfare Center, Newport, RI 02841

**Abstract:** In order to transmit energy in one direction, sonar flextensional transducers are combined into arrays of elements that are spaced a  $1/4$  wavelength apart. The directionality (front-to-back pressure ratio) is a modest of 6 dB. A single projector that is  $1/3$  wavelength in size and capable of developing unidirectional beams with front-to-back ratios greater than 20 dB that is independent of sound speed is described here. The directional Class VII “dogbone” flextensional is a modified version of an elliptical shaped Class IV flextensional having a concave shell rather than a convex one. The piezoelectric ceramic stack is a tri-laminar bar with two active sections separated by an inactive center section. By driving both sections of the stack in-phase, the shell is driven into omnidirectional radiation pattern. Driving each stack section 180 degrees out-phase causes a bending mode in the stack resulting in a dipole radiation pattern. By driving both sections using complex coefficients determined from the omnidirectional and dipole mode patterns, a cardioid directional radiation pattern is developed. Cardioid patterns are developed over an octave frequency band with a front-to-back pressure ratio of more than 50 dB. COMSOL Finite Element Analysis (FEA) code with Acoustics Module is used to predict in-water electroacoustic performance and compared with an experimental data.

**Keywords:** Transducer, Flextensional, Sonar, Piezoelectric, Directional, Cardioid, FEA

## 1. Introduction

Sonar transducers are used for transmitting and receiving acoustic energy for the purpose of detection and location of underwater objects. In figure 1, a ship is towing a variable depth sonar that contains sound projectors used to transmit the acoustic energy and a tethered line array of hydrophones used to receive the reflected sound waves from an underwater object<sup>1</sup>. These sound projectors are usually of a Class IV elliptical type flextensional sonar transducer that has proven to be rugged high power compact omnidirectional projectors<sup>2</sup>. In order to direct energy in a direction to minimize the

reverberation levels, avoid overloading the receiver line array preamplifiers, and removing the left-right ambiguity problem caused by symmetrical or Omnidirectional beams; these sound projectors are combined into two line arrays or two planar arrays of projector elements that are several wavelengths long and spaced a  $1/4$  wavelength apart, as shown in figure 2. Theoretically, two point sources spaced a  $1/4$  wavelength apart from one another with one of the sources driven 90 degrees out of phase with the other source will produce a cardioid type beam pattern with a null in the back that has a 3-dB down beamwidth of 180 degrees<sup>3</sup>, as shown in figure 3a. In practice this is not the case. Two Class IV flextensional transducers spaced  $1/4$  wavelength apart from one another with one of the sources driven 90 degrees out of phase will produce a front-to-back ratio of only 6 dB, as shown in figure 3b.

We will now describe the Directional Class VII Dogbone Flextensional Sonar Transducer projector which generates directional cardioid beams from a single transducer. The transducer is  $1/3$  wavelength in size with a front-to-back ratio greater than 20 dB and independent of sound speed. This transducer design is capable of generating an omnidirectional radiation beam pattern and a dipole radiation beam pattern which uses superposition to create a cardioid unidirectional beam. The synthesis is described in figure 4, where the omnidirectional source is represented as a positive pressure radiator and the dipole source is represented by positive and negative pressure radiators, which when combined form a cardioid pattern. Thus, the acoustic pressure output is doubled in one direction and nulled in the other direction. This type of pattern generates a directivity index (DI) of 4.8 dB and has a 3-dB down beamwidth of 130°. We are proposing that a single line array of these Directional Class VII dogbone flextensional transducers could replace a dual line array of Class IV flextensional transducers which will reduce weight, cost and increase front-to-back ratio, as shown in figure 5. We will show that cardioid type patterns can be developed over an octave frequency band with a predicted front (left) to back (right) pressure ratio

of more than 50 dB as compared with 6 dB for the 1/4 wavelength spaced apart projectors.

## 2. Description

This projector merges Directional Flextensional Class IV Transducer Technology<sup>4,5</sup> with that of a Class VII Dogbone Flextensional Transducer Technology<sup>6</sup>. We refer to this as the Directional Class VII Dogbone Flextensional Sonar Transducer, which produces enhanced motion on one surface and canceled motion on the second surface. The Class VII flextensional Sonar Transducer is referred to as a “dogbone” flextensional because of its similar shape to that which was originally described by Merchant in U.S. Patent 3,258,738 (28 June 1966). This Class VII flextensional is a modified Class IV shape having concave staves or beams radiating surfaces rather than convex staves or beams radiating surfaces (for comparison the two are shown in figure 6). This type of transducer has the advantages that all the surfaces of the shell radiate in phase and a positive compressive stress is maintained on the ceramic stack as the operation depth increases. The shell can support thinner walls, since hydrostatic pressures do not have to be overcome in order to keep the piezoelectric ceramic stack under compression as in a conventional Class IV transducer.

The piezoelectric ceramic stack is a trilaminar bender bar with two active sections separated by an inactive section which is inserted along the major axis of the shell. Driving both sides of the stack in-phase allows the shell to be driven into its conventional mode creating an omnidirectional radiation pattern. By driving each of the stack sides 180 degrees out-phase with one another causes a bending mode in the stack creating a dipole type (cosine) radiation pattern. By combining these two modes through superposition generates a cardioid type radiation pattern. The uniqueness of this transducer is its small size (less than a third of a wavelength) producing directional beam patterns at high acoustic output power from a single element, unlike 1/4 wavelength dual line arrays. COMSOL-Multiphysics finite element code Acoustics Module<sup>7</sup> with a Perfectly Matched Layer (*PML*) as a boundary condition is used to predict in-water electroacoustic performance (Impedance, TVR and Beam Patterns) of a Class VII dogbone transducer and compared with an omnidirectional 3 kHz Class VII flextensional transducer experimental prototype unit.

COMSOL is then used to predict the far field complex pressures of the omnidirectional and dipole modes which are used to determine the complex drive coefficients used to drive the transducer into the directional mode.

## 3. Model

Measured results from an omnidirectional 3 kHz Class VII flextensional transducer experimental prototype unit will be used to validate a 2-D FEA model before developing a directional Class VII flextensional transducer model. The experimental transducer has two shells and stacks electrically wired in parallel and two end plates separated by four long bolts. It is then encapsulated in a water tight polyurethane boot. Photos of the transducer Shell and Ceramic Stack are shown in figure 7a and encapsulated in figure 7b. Figure 8 shows the dimensions of the transducer model which is composed of a piezoelectric drive stack and vibrating shell. The stainless steel shell has thick rigid ends which the piezoelectric drive stack pushes against which in turn flexes the curved shell staves (or Beams). The staves are 4.32 mm thick and have an inner and outer radius of 85.85 mm and 90.17 mm respectively. The piezoelectric ceramic drive stack is composed of 30 PZT-8 U.S. Navy type III ceramic 33-mode plates that are each 2.54mm thick, 17.78 mm wide and 40.82 mm deep, two of which are unpoled and used for insulators on the ends. Figure 9 shows the 2-D FEA Stack Subdomain Settings and the Boundary Condition Settings for Piezoelectric Plane-Strain application FEA model, Plane-Stress FEA modeling for Piezoelectric application is not available. The glue joints and brass foil electrodes that are between each plate that are used to consolidate and wire the stack are not used here in the model. Instead, the piezoelectric material compliance matrix  $S_{33}^E$  was modified from  $13.5 \times 10^{-12} \text{ m}^2/\text{N}$  to  $21 \times 10^{-12} \text{ m}^2/\text{N}$  to account for the added compliance of the glue joints and foil electrodes, which lowers the stack in-air resonance from 22 kHz to that of the measured stack in-air resonance of approximately 17.3 kHz before it was inserted into the shell.

## 4. 2-D Ceramic Stack Model

As shown in figure 9 Stack Subdomain Settings, the ceramic plates are labeled PZT8U and PZT8D. This is to account for the electrical

polarization field polarity pointing to the direction of the positive electrode surface of the ceramic plate, thus the coordinate system must be rotated 180 degrees to one another. Figure 9c shows the electric potential and field arrows surface plot results with a positive rms voltage potential of 1 applied to the boundary settings listed in figure 9b. COMSOL does not allow direct extraction of electrical current under the piezoelectric application in order to calculate the electrical input impedance ( $Z=V/I$ ) or electrical input admittance ( $Y=I/V$ ) that are used to characterize sonar transducers. Thus, by integrating the Normal Current Density ( $nJ\_smppn$ ) or Displacement Current Density ( $Jdy\_smppn$ ) with respect to the ceramic plates surface area the inward current can be calculated. The Normal Current Density would be used when there are glue joints between plates or having an uncommon potential. Displacement Current Density would be used when there are no joints between plates and have a common potential, which is our case here. The expressions in equations (1) and (2) are the Displacement Current Density assigned to each of the positive potential (+V) surfaces listed in figure 9b. The Boundary Condition Settings the “up” and “down” in the equations represents the direction of the current flow that is associated with the chosen ceramic plates polarity field of the PZT8U and PZT8D plates.

$$IU = -(up(Jdy\_smppn))*z \quad (1)$$

$$ID = -(down(Jdy\_smppn))*z \quad (2)$$

The “z” represents the depth of the ceramic plates 40.82 mm and IU is the assigned the name for Equation (1) and ID is the assigned the name of equation (2), once these expression are integrated under COMSOL’s Integration Coupling Variable>Boundary Integration Variables menu Option. Therefore, by summing the magnitudes of both IU and ID is the total electrical current into the piezoelectric stack. The admittance magnitude is given by the sum of the magnitudes of both IU and ID divided by the applied electrical potential ( $V=1$ ), therefore the admittance magnitude is given by equation (3).

$$|Y|=I/V=abs(ID)+abs(IU) \quad (3)$$

Figure 10 shows the piezoelectric stack in-air modeled admittance magnitude response of the model shown in figure 9 using equation (3) compared with a measured stack that was used in

the prototype transducer shown in figure 7. Admittance is a complex quantity  $Y=G+jB$ , where G the conductance is the real part and B the susceptance is the imaginary part of the admittance, they are given in equations (4) and (5) for  $V=1$ ,

$$G= real(ID)-real(IU) \quad (4)$$

$$B= imag(ID)-imag(IU) \quad (5)$$

The IU is subtracted from ID to account for the opposite direction of the current flow that is associated with the chosen ceramic plate polarity, the order of subtraction maybe different for other models due to boundary condition choices. The capacitance is given by  $B/\omega$ , where  $\omega=2\pi f$  and therefore is given by equation (6)

$$C= (imag(ID)-imag(IU))/(2*\pi*freq) \quad (6)$$

where “freq” is the frequency in Hz. The low frequency 1 kHz capacitance of the stack predicted from the model was 64 nFd verses the measured 77 nFd. The models relative free dielectric constant  $\epsilon_r^T$  is 1000 verses that of the manufactures data sheet EDO EC-69 value of 1050.

## 5. 2-D Shell and Stack Model

The structural Subdomain Settings and the Boundary Condition Settings for the Shell and Piezoelectric Stack are shown in figure 11. The Shell material properties are of stainless steel and the piezoelectric stack is the same shown in figure 9. The shells are each 50.8 mm in height and the stacks are each 40.82 mm in height. The plane-strain application in COMSOL Acoustics Module allows a thickness of a material to be entered into the z- axes, which otherwise it would be a unit or 1 meter thickness. For the Shell/Stack model 0.1016 m was entered for shell thickness and 0.08164 m for stack thickness, 1 meter and 0.80354 meters for shell and stack respectively would also work. For the proper current results the “z” value in equations 1 and 2 is 0.08164 m. The fluid Subdomain Settings and the Boundary Condition Settings for pressure acoustics (acpr) application mode are shown in figure 12. The fluid loading is in two parts the inside water boundary and the outside boundary the Perfectly Matched Layer (*PML*). The water boundary contains the acoustic properties, the density and speed of sound of the

fluid and is two wavelengths in radius at 3 kHz or 1 meter and is considered a far-field radiation condition, this is where the acoustic information is contained. The *PML* is the radiation condition for perfectly absorbing plane, cylindrical and spherical waves and absorbs incident radiation without producing reflections, here the model is 0.5 meters or one wavelength wide. The *PML* is a cylindrical type loading for this 2-D geometry model, thus the acoustic pressure will decrease cylindrically in the radial and z-axis direction. At the interface between the water and shell an outward pressure  $-p$  in terms of force per unit area is applied as a Load around the surface of the shell and is given by equations (7) and (8). A normal acceleration  $a_n$  is applied around the surface of the shell in equation (9); this boundary condition is used to couple the acoustic domain to structural domain. A far field  $p_{far}$  condition is applied around the outer boundary of the *PML*.

$$F_x = -p * n_x_{smppn} \quad (7)$$

$$F_y = -p * n_y_{smppn} \quad (8)$$

$$a_n = n_x_{smppn} * u_{tt_{smppn}} + n_y_{smppn} * v_{tt_{smppn}} \quad (9)$$

The 2-D FEA Fluid and Shell/Stack Mesh is shown in figure 13, the mesh contains 16312 triangular elements. The typical rule of thumb for element size is greater than five elements per wavelength<sup>7</sup>. This is to allow higher frequency calculations and as can be seen we are far greater than that. COMSOL application scalar variables pressure reference  $p_{ref}$  should be change to 1E-6 Pa this is the acoustic sound pressure reference level for water. Also both the excitation frequency variables  $freq_{smppn}$  and  $freq_{acpr}$  should contain the expression  $freq$  which will couple the acoustic domain and structural domain together for performing a frequency response and a time harmonic analysis. COMSOL acoustic sound pressure level (SPL),  $L_p$  at some point in the water acoustic pressure field is given by equation (10)

$$SPL = 10 \log_{10} \left( \frac{pp^*}{2 p_{ref}^2} \right) \quad (10)$$

where  $p_{ref}$  is the acoustic sound pressure reference level for water 1 uPa. Here the pressure  $p$  is a peak value since the 2 in the denominator normalizes  $pp^*$  to a rms value. The more common form in terms of rms pressure is

$$SPL = 20 \log_{10} \left( \frac{p_{rms}}{p_{ref}} \right) \quad (11)$$

Transmit voltage response (*TVR*) is an important transducer calibration parameter that describes the *SPL* of a transducer at 1 meter distance when driven with 1 volt rms over a frequency band of interest and has the units of *dB/1uPa/Vrms at 1m*. Thus to determine the proper *TVR* level when using COMSOL's *SPL* function a voltage potential of  $\sqrt{2}$  Volts is used instead of 1 Volt, since a peak voltage will generate a peak pressure. If a voltage potential of 1 Volt was used, 3 dB would be needed to be added to the *SPL*. As discussed earlier the 2-D model has cylindrical loading, thus both the acoustic pressure will decrease cylindrically in the radial and z-axis direction. The *TVR* given in equation (12) accounts for cylindrical loading effects of both the radial and z-axis directions

$$TVR = SPL - 10 \log_{10}(1/h) - 10 \log_{10}(1/r) \quad (12)$$

where  $h$  is the transducer height in the z-direction and  $r$  is the radial distance pressure point. The transducer is 0.1016 m in height and radial distance pressure is 1 meter. The *TVR* equation is now  $TVR = SPL - 9.93 \text{ dB}$ .

## 6. In-Water Results

The in-water measured and modeled transmit voltage response using equation (12) is shown in figure 14. The resonance at 3 kHz is the first fundamental flexural mode of the transducer with a design of operation of 2.5 kHz to 5 kHz. The second resonance at approximately 10 kHz is the breathing (Hoop) mode of the Class VII shell. This mode happens when the circumference of the ring (beams) are equal to the wavelength in the shell material. The in-water measured and modeled conductance  $G$  response using equation (4) and susceptance  $B$  response using equation (5) are shown in figures 15 and 16 respectively for voltage potential of 1 Volt applied to the piezoelectric stack. The modeled response resonant peaks in the conductance response are lower than in the measured. This is a result the cylindrical loading which will overly dampen the model versus that of spherical loading. The measured and modeled acoustic radiation beam patterns at 3 kHz, 5 kHz and 9.6 kHz are shown in figure 17. The acoustic beam patterns in COMSOL are recorded by plotting the *SPL* verses bearing angle

( $\text{atan2}(y,x)$ ) around the shell at the radial distance pressure of 1 meter.

## 7. Directional Dogbone Model

The directional dogbone model shown in figure 18 is a slight modification of the model shown in figure 8. Here the piezoelectric ceramic stack is divided into two active sections, a Side-A and a Side-B separated by an inactive section. This will allow the transducer to be driven into the dipole and directional modes. This is demonstrated in figure 19 by applying the same voltage potential to both sides of the stack. This allows the shell to be driven into its conventional mode where both beams flex in and out with the same phase. This will create an omnidirectional radiation pattern, see figure 19a. Applying opposite voltage potentials to each of the stack sides will cause a bending mode in the stack which will cause the beams to flex out of phase with each other creating a dipole type (cosine) radiation pattern, see figure 19b. By combining these two modes through superposition by driving the stacks with complex voltage potential coefficients will minimize motion on one side and enhanced motion on the other side. This will generate a cardioid type radiation pattern.

## 8. Complex Voltage Potential Coefficients

The complex voltage potential drive coefficients for the transducer to generate a cardioid type radiation pattern are determined from acoustic *SPL* amplitude and phase of each of the modes in the far-field and then combining them. The omnidirectional mode is excited by applying 1 volt to sides-A ( $E_a=1$ ) and 1 volt to side-B ( $E_b=1$ ); this generates a far-field complex sound pressure  $P_o$ . The dipole mode is excited by applying 1 volt to sides-A ( $E_a=1$ ) and -1 volt to side-B ( $E_b=-1$ ); this generates a far-field complex sound pressure  $P_d$ . The two pressures should always be at the same angular position. The two-mode synthesis for determining the complex voltage potential drive coefficients  $E_a$  and  $E_b$  in algebraic form is as follows:

$$E_a = (P_d + P_o) / P_d = 1 + R, \quad (13)$$

$$E_b = (P_d - P_o) / P_d = 1 - R \quad (14)$$

where  $R = P_o / P_d$ . For enhanced pressure on side-A the omnidirectional pressure is added to the dipole pressure as shown in equation (13)

and for a null on side-B of shell the omnidirectional pressure is subtracted from the dipole pressure as shown in equation (14). Since each of the modes produces different *SPL*'s, equations (13) and (14) are normalized by the dipole mode pressure  $P_d$ . Also, since these equations contain complex pressures with different amplitude and phases, the omnidirectional pressure phase is referenced to the dipole pressure phase. The ratio of equations (13) and (14) is given by equation (15)

$$E_a / E_b = 1 + R / 1 - R \quad (15)$$

which normalizes the voltage potential of ceramic stack side-A to that of ceramic stack side-B in terms of a complex quantity or amplitude and phase quantity. Figure 20 shows the a) amplitude pressure and b) phase plots angle in the omnidirectional and dipole modes that were used to calculate the complex voltage potential coefficients at 3 kHz. The peak omnidirectional pressure is  $P_{pk} = 32.73 \text{ Pa}$  and phase is  $\phi_o = 84.86^\circ$ , therefore the rms pressure is  $P_{rms} = 23.15 \text{ Pa}$  and the *SPL* is  $147.29 \text{ dB}$  using equation (11) and the *TVR* is  $137.36 \text{ dB}/1\mu\text{Pa}/\text{V}@1\text{m}$  using equation (12). The peak dipole pressure is  $P_{pk} = 6.97 \text{ Pa}$  and phase is  $\phi_d = -144.36^\circ$ , therefore the rms pressure is  $P_{rms} = 4.93 \text{ Pa}$  and the *SPL* is  $133.86 \text{ dB}$  using equation (11) and the *TVR* is  $123.93 \text{ dB}/1\mu\text{Pa}/\text{V}@1\text{m}$  using equation (12). These *TVR*'s were then converted back to pressures, then *R* is computed and the ratio of  $E_a/E_b$  is solved. The reasoning for computing the *TVR* is this is the most commonly measured quantity on underwater sonar transducers. The complex voltage potential coefficients for 2, 3 and 4 kHz are shown in Table I. The complex values were applied instead of amplitude and phase, side-A voltage potential is  $E_a = (-0.721 - j*0.244) * 1.414$  and side-B voltage potential is  $E_b = 1 * 1.414$  at 3 kHz.

**Table I. Complex Voltage Potential Coefficients for 2, 3 and 4 kHz.**

Freq (kHz)	Omn TVR (dB)	Omn Phase (deg)	Dipole TVR (dB)	Dipole Phase (deg)	R Mag	R Phase (deg)	EaEb Mag	EaEb Phase (deg)	Ea Real (dB)	Ea Im (dB)	Ea Vrms	Eb Vrms	Direct TVR (dB)	Direct Phase (deg)
2	127.88	7.82	136.96	-118.81	0.356	-111.09	0.793	-37.73	-0.621	-0.481	1	1	132.96	61.4
3	132.69	84.97	123.93	-144.36	4.694	-223.23	0.703	-170.59	-0.271	-0.244	1	1	128.23	67.4
4	134.37	160.29	124.62	-32.35	3.073	-152.64	0.520	-170.90	-0.514	-0.082	1	1	128.23	67.4

The modeled pressure surface and *SPL* surface plots in the omnidirectional, dipole and directional modes at 3 kHz are shown in figure 21a and 21b respectively. The molded beam pattern omnidirectional, dipole and directional modes at 3 kHz are shown in figure 22a, 22b and 22c respectively. Using these coefficients in

Table I will point the beam to side-B direction instead of side-A direction. This may be caused by the dipole beam patterns lobe on side-B 180 degrees out-of phase with side -A lobe as shown in figure 4, for presentation purposes the cardioid beams were reversed to point to side-A direction in figures 21 and 22. The cardioid type beam pattern generated in figure 22c has a 67.6 dB front-to-back ratio (or deep back null) and a -3 dB beamwidth of 142.5 degrees. Cardioid beam pattern were generated from 1 kHz to 6 kHz in steps of 100 Hz. The lowest front-to-back ratio is 56.5 dB and -3 dB beamwidth ranged from 131 degrees at 1 kHz to 164 degrees at 4.5 kHz. The TVR omnidirectional, dipole and directional modes from 1 kHz to 6 kHz are plotted in figure 23 for comparison. The back null side of the directional mode is also plotted to show the relative front-to-back ratio.

The oceans sound speed and density profiles<sup>8</sup> both vary with water depth. Thus it would be interesting to see what would happen to the front-to-back ratio when using the same coefficients that were determined with the sound speed 1500 m/s and density 1000 kg/m<sup>3</sup> at 3 kHz. Figure 24 shows the front-to-back ratio comparison between two element Class IV flextensional transducers spaced 1/4 wavelength apart shown in figure 3b and the Class VII Directional Dogbone flextensional using the 3 kHz coefficients in Table I for different sound speeds while keeping the density constant. The other case is varying the sound speed while keeping the characteristic impedance (density times sound speed) the same  $\rho \cdot c = 1.5 \times 10^6$  Pa-m/s. The two element Class IV flextensionals had a constant front-to-back ratio of 6 dB from 1300 to 1700 m/s, while the dogbone had a greater than 20 dB front-to-back ratio for both cases.

## 9. Conclusions

COMSOL-Multiphysics finite element code and Acoustics Module with a *PML* as a boundary condition is used to predict in-water electroacoustic performance (Impedance, TVR and Beam Patterns) of a directional Class VII dogbone transducer. The model was compared with an omnidirectional 3 kHz Class VII flextensional transducer experimental prototype unit with good agreement. COMSOL is then used to predict the far field complex pressures of the omnidirectional and dipole modes which are then used to determine the complex drive

coefficients used to drive the transducer into the directional mode that generated cardioid type beam patterns. We showed that cardioid type patterns can be developed over an octave frequency band with a predicted front-to-back pressure ratio of more than 50 dB as compared with 6 dB for the 1/4 wavelength spaced apart projectors. Thus a single line array of these Directional Class VII dogbone flextensional transducers could replace a dual line array of Class IV flextensional transducers, which will reduce weight, cost and increase front-to-back ratio.

## 10. Reference

1. X. Lurton, "An Introduction to Underwater Acoustics, Principles and Applications," Springer, New York (2002).
2. K. D. Rolt, "History of the flextensional electroacoustic transducer," J. Acoust. Soc. Am., Vol. 87, 1340-1349 (1990).
3. C. H. Sherman and J. L. Butler, "Transducers and Arrays for Underwater Sound," Springer, New York (2007).
4. S.C. Butler, A.L. Butler and J.L. Butler, "Directional Flextensional Transducer," J. Acoust. Soc. Am., Vol. 92, No. 5, November 1992.
5. S.C. Butler, J.L. Butler, A.L. Butler and G.H. Cavanagh, "A Low Frequency Directional Flextensional Transducer and Line Array," J. Acoust. Soc. Am., Vol. 102, No. 1, July 1997.
6. S. C. Butler and J. F. Lindberg, "A 3-kHz Class VII Flextensional Transducer," J. Acoust. Soc. Am. 101, 3164 (1997).
7. Acoustic Module User's Guide, COMSOL Multiphysics 3.5a (2008).
8. R. J. Urick, "Principles of Underwater Sound," 3<sup>rd</sup> edition, Peninsula Publishing, Los Altos, CA (1983).

# 11. Acknowledgements

The author would like to thank Jan F. Lindberg of the Office of Naval Research for his support on this project and to the technical staff at the Naval Undersea Warfare Center. This work was sponsored by the Office of Naval Research, (S&T) Science & Technology program.

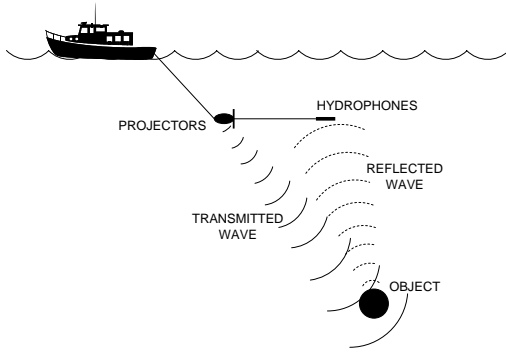


Figure 1. Sonar uses Transmitted and Reflected Sound Waves to Locate Underwater Objects

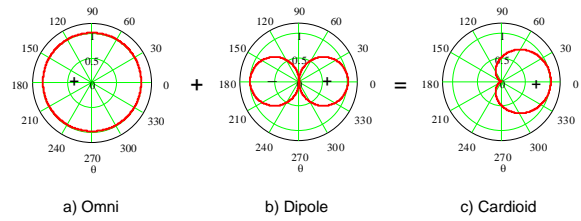


Figure 4. Synthesis of a Directional Flextensional

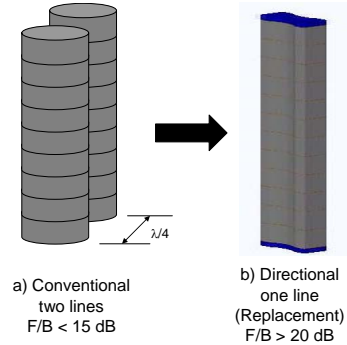


Figure 5. Two Line Arrays of Projector Elements that are Several Wavelengths Long and Spaced a 1/4 Wavelength Apart Replaced by One Line Array of Directional Dogbone Transducers Producing a Front-to-back ratio greater than 20 dB.

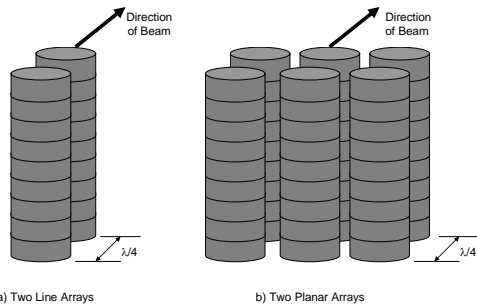


Figure 2. Two Line Arrays and Planar Arrays of Projector Elements that are Several Wavelengths Long and Spaced a 1/4 Wavelength Apart.

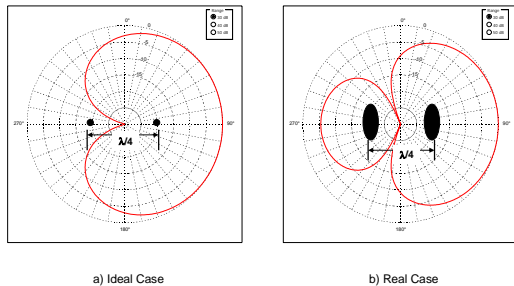


Figure 3. Modeled Beam Patterns for Two sources spaced a 1/4 wavelength apart with one of the sources driven 90 degrees out of phase with the other sources, a) for Point Source Element and b) Real Case Flextensional Elements.

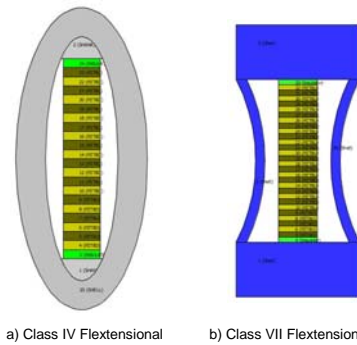


Figure 6. Class IV Flextensional Transducer and Class VII "Dogbone" Flextensional Transducer

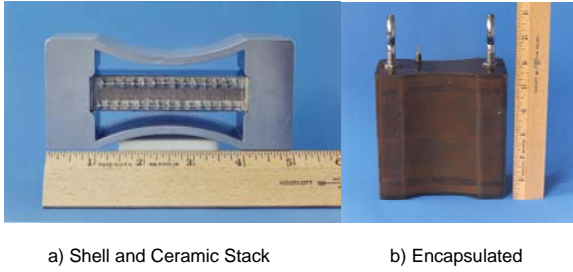


Figure 7. Class VII "Dogbone" Flextensional Sonar Transducer, Shell and Ceramic Stack and b) Encapsulated

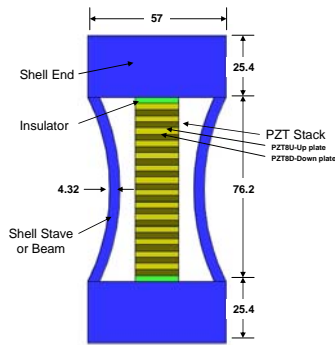


Figure 8. Class VII Dogbone Flextensional Sonar Transducer Dimensions in mm.

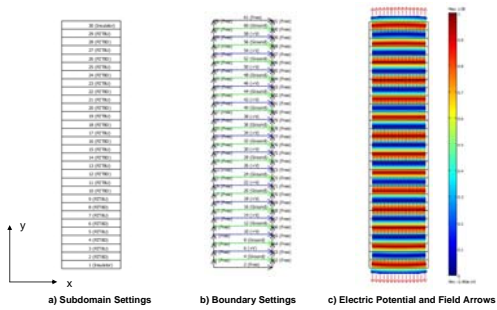


Figure 9. COMSOL Stack a) Subdomain Settings and b) Boundary Settings for Piezo Plane Strain (smppn) application and c) Electric Potential and Field Arrows results

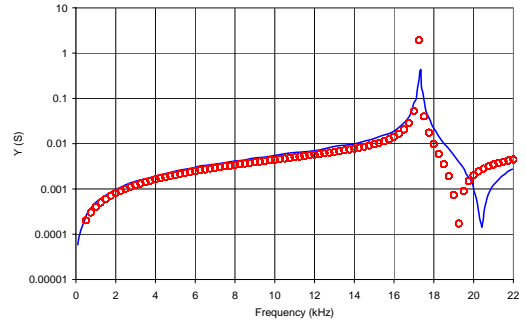


Figure 10. Piezoelectric Stack In-air Admittance Magnitude Response Measured (\_\_\_\_) and COMSOL FEA Modeled (oooo)

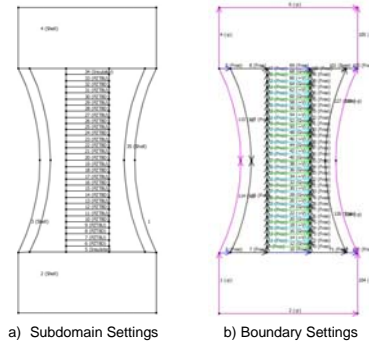


Figure 11. COMSOL Shell and Stack a) Subdomain Settings and b) Boundary Settings For Piezo Plane Strain (smppn) application

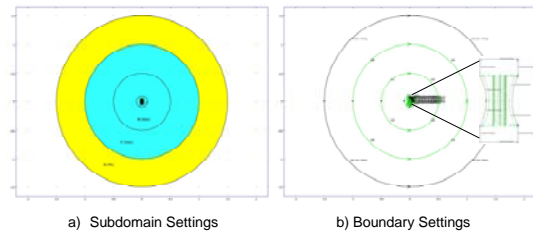


Figure 12. COMSOL Fluid, Shell and Stack a) Subdomain Settings and b) Boundary Settings for Pressure Acoustics (acpr) application



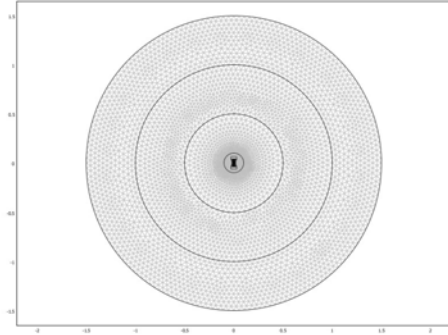


Figure 13. COMSOL 2-D FEA Fluid and Shell/Stack Mesh

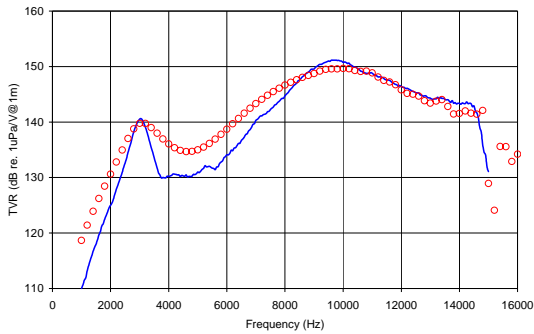


Figure 14. Transmit Voltage Response Measured (\_\_\_\_) and COMSOL Modeled (oooo)

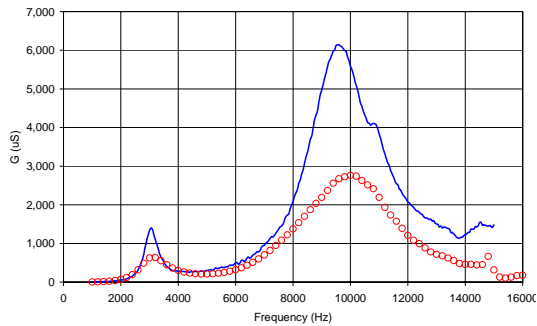


Figure 15. In-water Conductance Response Measured (\_\_\_\_) and COMSOL FEA Modeled (oooo)

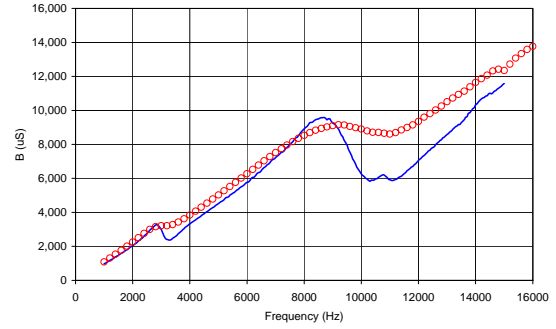


Figure 16. In-water Susceptance Response Measured (\_\_\_\_) and COMSOL Modeled (oooo)

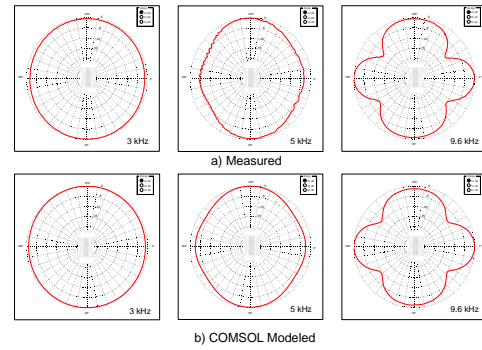


Figure 17. Beam Patterns in Omnidirectional Mode a) Measured and b) COMSOL Modeled at 3 kHz, 5 kHz and 9.6 kHz

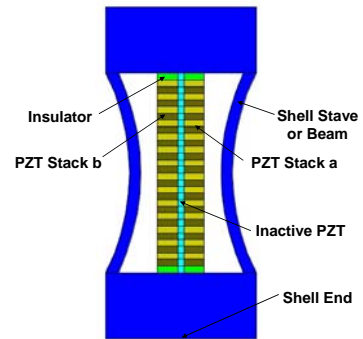


Figure 18. Directional Dogbone Flextensional Sonar Transducer

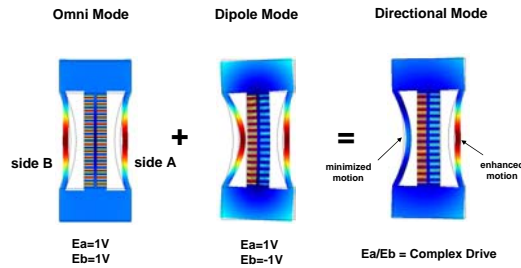


Figure 19. COMSOL FEA Piezoelectric Ceramic Stack Electric Fields and Displacement Shell and Stack Modes for Omnidirectional, Dipole and Directional Modes at 3 kHz

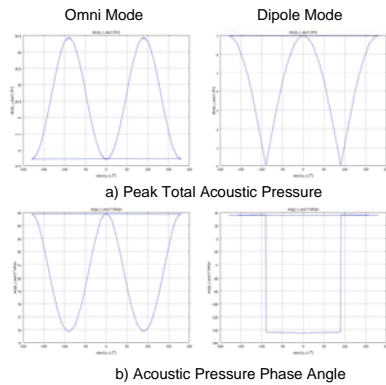


Figure 20. COMSOL FEA Molded a) Peak Acoustic Pressure and b) Acoustic Pressure Phase Angle in the Omnidirectional and Dipole Modes at 3 kHz

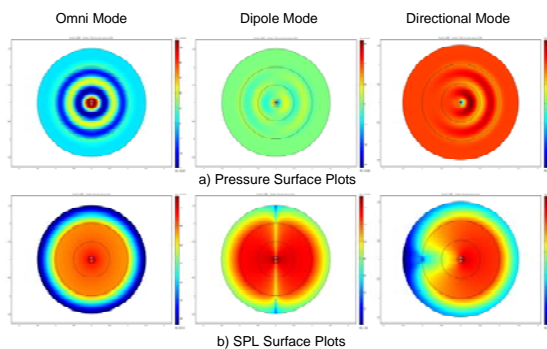


Figure 21. COMSOL FEA Molded a) Pressure and b) SPL Surface Plots in the Omnidirectional, Dipole and Directional Modes at 3 kHz

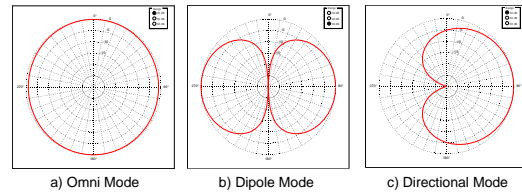


Figure 22. COMSOL FEA Molded Beam Pattern a) Omnidirectional, b) Dipole and c) Directional Modes at 3 kHz

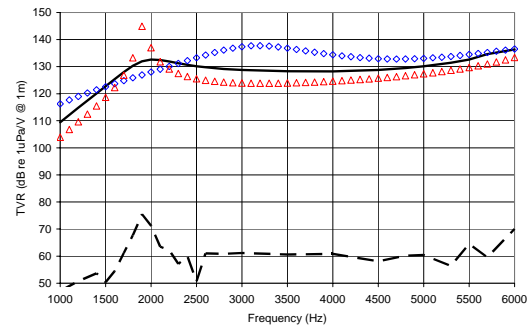


Figure 23. COMSOL FEA Modeled Transmit Voltage Response Omnidirectional Mode (◇◇◇◇), Dipole Mode (△△△△), Front Side Directional Mode (\_\_\_\_) and Back Side Directional Mode (-----)

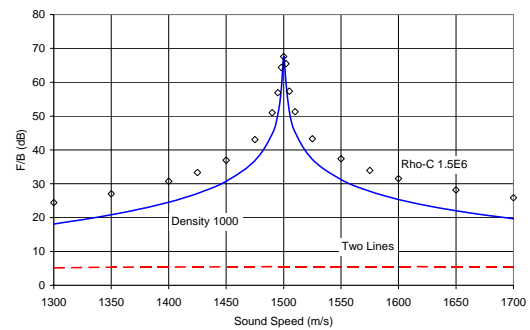


Figure 24. Front-to-back Ratio Comparison Between Two Lines (-----) and Directional Dogbone (\_\_\_\_) and Constant Characteristic Impedance (◇◇◇◇) using the 3 kHz Coefficients for different Sound Speeds.